lowed by a more controlled set of stimulation conditions. The reverse-correlation method could be further supported by a more quantitative analysis, e.g., by a binomial probability estimation using an objective, binary rating of the presence of specific stimuli (e.g., faces) in each frame of the various movies.

References and Notes

1. W. A. Press, A. A. Brewer, R. F. Dougherty, A. R. Wade, B. A. Wandell, *Vision Res.* **41**, 1321 (2001).
2. R. B. H. Tootell et al., *J. Neurosci.* **17**, 7060 (1997).
3. K. Grill-Spector, *Curr. Opin. Neurobiol.* **13**, 159 (2003).
4. U. Hasson, M. Harel, I. Levy, R. Malach, *Neuron* **37**, 1027 (2003).
5. A. Ishai, L. G. Ungerleider, A. Martin, H. L. Schouten, J. V. Haxby, *Proc. Natl. Acad. Sci. U.S.A.* **96**, 9379 (1999).
6. D. L. Ringach, M. J. Hawken, R. Shapley, *J. Vis.* **2**, 12 (2002).
7. E. T. Rolls, N. C. Aggelopoulos, F. S. Zheng, *J. Neurosci.* **23**, 339 (2003).
8. D. L. Sheinberg, N. K. Logothetis, *J. Neurosci.* **21**, 1340 (2001).
9. T. Hartley, E. A. Maguire, H. J. Spiers, N. Burgess, *Neuron* **37**, 877 (2003).
10. E. A. Maguire et al., *Science* **280**, 921 (1998).
11. J. M. Zacks et al., *Nat. Neurosci.* **4**, 651 (2001).
12. A. Bartels, S. Zeki, *Hum. Brain Mapp.* **21**, 75 (2004).
13. L. Vincenzoni, S. Leone, *The Good, the Bad, and the Ugly*, S. Leone, Director, 161 min, Metro-Goldwyn Mayer (MGM), 1966.
14. Materials and methods are available on *Science* Online. BrainShow.exe is available at www.weizmann. ac.il/neurobiology/labs/malach/ReverseCorrelation.
15. In order to search for correlation between two corresponding regions across subjects (intersubject correlation), we first aligned all brains into Talairach coordinate system and used a Gaussian filter of 12 mm full width at half maximum value (FWHM) to the data [similar results were obtained with the use of 8 mm FWHM (17)]. To remove preprocessing artifacts, we excluded the first and last 10 time points of the experiment from the analysis. We then used the time course of each voxel of the source subject as a GLM predictor for modeling the activity in the corresponding voxel of the target subject. Only voxels whose *P* value was no more than 0.05 (corrected) were considered significant.
16. P. Janata et al., *Science* **298**, 2167 (2002).
17. U. Hasson, Y. Nir, I. Levy, G. Fuhrmann, R. Malach, unpublished data.
18. J. P. Jones, L. A. Palmer, *J. Neurophysiol.* **58**, 1187 (1987).
19. For the reverse correlation, each given time course was z-normalized and smoothed with a moving average of three time points. A *t* test was applied to each time point along the averaged time course, and only time points that were significantly different (*P* < 0.05) from the average mean value (i.e., 0) were included in the analysis (colored in Figs. 3 and 4). With the use of the inhouse "Brain Show" software, we then reconstructed a short "movie" composed of the frames that led to the highest BOLD signal in each specific region, assuming our standard hemodynamic lag of 3 s. We then examined those movies in an attempt to evaluate each region's functional specialization under natural viewing conditions.
20. To remove the nonselective component from the movie data set for the region-specific time course, we z-normalized the common "time course" of each subject (Fig. 2B), smoothed it with a moving average of three time points, and then used it as a GLM predictor, which was fitted to the entire data set of the subject. The residual time course (which was not explained by the predictor) was saved as a new time course.
21. N. Kanwisher, J. McDermott, M. M. Chun, *J. Neurosci.* **17**, 4302 (1997).
22. J. V. Haxby, E. A. Hoffman, M. I. Gobbini, *Trends Cognit. Sci.* **4**, 223 (2000).
23. G. K. Aguirre, E. Zarahn, M. D'Esposito, *Neuron* **21**, 373 (1998).
24. R. Epstein, N. Kanwisher, *Nature* **392**, 598 (1998).
25. To view all frames associated with the peaks of activation in the fusiform face-related, building-related, and PCS regions, use the DVD of (13) and BrainShow.exe (14).
26. P. E. Downing, Y. Jiang, M. Shuman, N. Kanwisher, *Science* **293**, 2470 (2001).
27. M. S. Beauchamp, K. E. Lee, J. V. Haxby, A. Martin, *Neuron* **34**, 149 (2002).
28. A. Puce, T. Allison, S. Bentin, J. C. Gore, G. McCarthy, *J. Neurosci.* **18**, 2188 (1998).
29. E. A. Hoffman, J. V. Haxby, *Nat. Neurosci.* **3**, 80 (2000).
30. A. R. Damasio, *The Feeling of What Happens: Body and Emotion in the Making of Consciousness* (Harcourt Brace, New York, ed. 1, 1999).
31. J. V. Haxby et al., *Science* **293**, 2425 (2001).
32. H. D. Critchley et al., *Brain* **126**, 2139 (2003).
33. J. J. DiCarlo, J. H. Maunsell, *Nat. Neurosci.* **3**, 814 (2000).
34. K. Grill-Spector et al., *Neuron* **24**, 187 (1999).
35. M. Ito, H. Tamura, I. Fujita, K. Tanaka, *J. Neurophysiol.* **73**, 218 (1995).
36. J. A. Brefczynski, E. A. DeYoe, *Nat. Neurosci.* **2**, 370 (1999).
37. K. M. O'Craven, P. E. Downing, N. Kanwisher, *Nature* **401**, 584 (1999).
38. R. B. Tootell et al., *Neuron* **21**, 1409 (1998).
39. G. Rizzolatti, L. Fogassi, V. Gallese, *Curr. Opin. Neurobiol.* **7**, 562 (1997).
40. G. Rizzolatti, L. Fadiga, V. Gallese, L. Fogassi, *Brain Res. Cognit. Brain Res.* **3**, 131 (1996).
41. S. Cochin, C. Barthelemy, S. Roux, J. Martineau, *Eur. J. Neurosci.* **11**, 1839 (1999).
42. A. Dijksterhuis, J. A. Bargh, in *Advances in Experimental Social Psychology*, M. P. Zanna, Ed. (Academic Press, San Diego, CA, 2001), vol. 33, pp. 1–40.
43. J. M. Kilner, Y. Paulignan, S. J. Blakemore, *Curr. Biol.* **13**, 522 (2003).
44. This study was funded by the Benoziyo Center. We thank the Wohl Institute for Advanced Imaging in the Tel-Aviv Sourasky Medical Center; M. Behrmann, K. Grill-Spector, G. Avidan, M. Peleg, and S. Gilaie-Dotan for fruitful discussions and comments; R. Goebel and D. Paserman for helping with the intersubject analysis; M. Harel for three-dimensional brain reconstructions; E. Okon for technical assistance; E. Malach for programming the "brain-show" reverse-correlation analysis tool; and R. Mukamel for software development. We thank C. Eastwood and H. Grimaldi for kindly providing us with permission to use the frames.

The Wheat *VRN2* Gene Is a Flowering Repressor Down-Regulated by Vernalization

Liuling Yan,[1]* Artem Loukoianov,[1] Ann Blechl,[2] Gabriela Tranquilli,[1]† Wusirika Ramakrishna,[3] Phillip SanMiguel,[4] Jeffrey L. Bennetzen,[5] Viviana Echenique,[1]‡ Jorge Dubcovsky[1]*§

Plants with a winter growth habit flower earlier when exposed for several weeks to cold temperatures, a process called vernalization. We report here the positional cloning of the wheat vernalization gene *VRN2*, a dominant repressor of flowering that is down-regulated by vernalization. Loss of function of *VRN2*, whether by natural mutations or deletions, resulted in spring lines, which do not require vernalization to flower. Reduction of the RNA level of *VRN2* by RNA interference accelerated the flowering time of transgenic winter-wheat plants by more than a month.

Common wheat (*Triticum aestivum* L.) is one of the primary grains consumed by humans and is grown in very different environments.

[1]Department of Agronomy and Range Science, University of California, Davis, CA 95616, USA. [2]U.S. Department of Agriculture–Agricultural Research Service, Albany, CA 94710, USA. [3]Department of Biological Sciences, Michigan Technological University, Houghton, MI 49931, USA. [4]Purdue University Genomics Core, Purdue University, West Lafayette, IN 47907, USA. [5]Department of Genetics, University of Georgia, Athens, GA 30602, USA.

*These authors contributed equally to this work.
†Present address: Instituto Recursos Biológicos, Instituto Nacional de Tecnología Agropecuaria, (1712) Castelar, Buenos Aires, Argentina.
‡Present address: Consejo Nacional Investigaciones Cientificas y Tecnicas Departamento de Agronomía, Universidad Nacional del Sur, 8000 Bahía Blanca, Argentina.
§To whom correspondence should be addressed. E-mail: jdubcovsky@ucdavis.edu

This wide adaptability has been favored by the existence of wheat varieties with different growth habits. Winter wheats require a long exposure to low temperatures in order to flower (vernalization) and are sown in the fall, whereas spring wheats do not require vernalization and can be planted in the spring or fall. The genes from the vernalization pathway prevent flower development during the winter, providing protection for the temperature-sensitive floral organs against the cold. *VRN1* and *VRN2* are the central genes in the vernalization pathway in wheat, barley, and other temperate cereals. These two genes have strong epistatic interactions and are likely part of the same regulatory pathway (*1*, *2*). In both diploid wheat (*T. monococcum* L.) and barley, *VRN1* is dominant for spring growth habit, whereas *VRN2* is dominant for

winter growth habit. Similar epistatic interactions and map locations indicate that wheat and barley vernalization genes are orthologous (*3*, *4*).

The *VRN1* gene from wheat is similar to the *Arabidopsis* meristem identity gene *APETALA1* (*AP1*) (*5*), which initiates the transition from the vegetative to the reproductive apex. Natural allelic variation at the *AP1* locus is associated with differences in vernalization requirement in wheat but not in *Arabidopsis* (*5*). In *Arabidopsis*, natural variation for vernalization requirement has arisen through the generation of nonfunctional or weak *FRI* and *FLC* alleles (*6*). The *Arabidopsis FLC* gene is a repressor of flowering that integrates the signals from the autonomous flowering pathway with those from extended cold treatment. *FRI* elevates expression of *FLC* to levels that inhibit flowering, whereas vernalization produces a permanent down-regulation of *FLC* and induces flowering (*7–9*).

Induced mutations have been used to identify additional vernalization genes in *Arabidopsis*. *VIN3* is induced by vernalization and is involved in the transient repression of *FLC* by histone deacetylation (*10*). Two additional *Arabidopsis* genes, designated *VRN1* and *VRN2*, are required to keep *FLC* in its repressed state, but not for its initial repression by cold (*11*, *12*). *Arabidopsis VRN1* and *VRN2* are different from the wheat genes with the same names. The *VRN1* and *VRN2* names are standard designations for the wheat vernalization loci, and we will use them hereafter to refer to the cereal genes.

Positional cloning of the wheat vernalization gene VRN2. The *VRN2* gene was initially mapped on chromosome 5A, in a small F_2 population from the cross between spring (no. DV92) and winter (no. G3116) accessions of diploid wheat *T. monococcum* (*4*). We used the same parental lines to develop a high-density map based on 5698 gametes (*13*). Screening of this population with *VRN2* flanking markers *NUCELLIN* and *UCW22* resulted in the identification of 18 recombination events within this region (Fig. 1) (*13*). Progeny tests for vernalization requirement were performed for these 18 plants. We generated additional markers from the bacterial artificial chromosome (BAC) clones included in the physical map (Fig. 1) and defined the location of the two crossovers that flank *VRN2* (figs. S2 to S4). The *VRN2* gene was mapped into a 0.04-cM interval flanked by the restriction fragment length polymorphism (RFLP) marker *UCW22* and polymerase chain reaction (PCR) marker *UCW2.1* (Fig. 1).

Markers *UCW22* and *UCW2.1* were used to screen the BAC library of *T. monococcum* accession no. DV92 (*14*). A physical map of the *VRN2* region was constructed by chromosome walking (Fig. 1). Overlapping BACs 258C22, 301G15, 405L8, and 455C17 were sequenced [438,828 base pairs (bp)], annotated, and deposited in GenBank (accession no. AY485644). We also sequenced orthologous BAC 615K1 from

barley variety Morex (accession no. AY485643) and BAC 49F5 from rice variety Nipponbare (accession no. AF485811).

Eight genes and one pseudogene were detected within the sequenced region, indicating a gene density of one gene per 55 kb and a ratio between genetic and physical distances of ∼1.7 Mb/cM. Five of these genes were found in the same order and orientation in the barley BAC and three in the rice BAC, confirming the colinearity of this region among cereals (Fig. 1). The closest common genes flanking the *VRN2* gene, *PDS* and *SNF2P*, were 7 kb apart in rice, 26 kb apart in barley, and 328 kb apart in *T. monococcum* (Fig. 1).

The sequences from markers *UCW22* and *UCW2.1* flanking the *VRN2* gene in the genetic map (Fig. 1) were used to delimit a 315-kb candidate region within AY485644. About 75% of this sequence was annotated as repetitive elements. Within the nonrepetitive region, only three genes were completely linked to *VRN2*. The first gene, designated *AY485644.3*, encoded a predicted 254–amino acid protein that was 87% and 96% similar to the putative orthologous proteins in the colinear BACs from rice and barley, respectively (Fig. 1). The function of gene *AY485644.3* is currently unknown.

The other two genes completely linked to *VRN2* encoded proteins that were 76% identical, suggesting a duplication event that occurred ∼14 ± 3 million years ago (supporting online text). These two proteins had similarities with CO and CO-like proteins of *Arabidopsis* ($E = 2e^{-11}$, where *E* is the expected number of hits by chance and *e* is the mathematical constant) and rice (accession no. AP005307, OsI, $E = 3e^{-16}$; accession no. AAL79780, OsH, $E = 2e^{-16}$). This similarity was restricted to the 43 amino acids of the CO, CO-like, and TOC1 (CCT) domain present in all these proteins (fig. S10). This domain determines the nuclear localization of *CO*, the key gene in the *Arabidop-*

sis photoperiod pathway (*15*, *16*), and may have a similar function in these two genes. We named these two genes *ZCCT1* and *ZCCT2*, because of the presence of a putative zinc finger in the first exon and of the CCT domain in the second exon.

Evolutionary relationships between the *ZCCT* and *CO*-like genes. We isolated similar *ZCCT* genes from the A genome of tetraploid wheat (accession nos. AY485979 and AY485980) and from winter barley variety Diarokkaku (accession nos. AY485977 and AY485978) and compared their CCT domains with those from other *CO*-like genes (fig. S10). We performed a Neighbor Joining cluster analysis using the CCT motifs from the ZCCT proteins and from members of each of the four major classes (I to IV) of CO-like proteins (*17*) (fig. S11). CCT motifs from Group III (At-COL9 and OsN) were used as an outgroup. The ZCCT proteins formed a separate group that did not include any rice or *Arabidopsis* protein. This group was related to Group IV proteins (HvCO9, OsI, and OsH), which included proteins only from grass species. Proteins from both *Arabidopsis* and grass species were present in the separate Groups I (AtCO and OsHD1) and II (AtCOL6 and OsJ), including proteins involved in the regulation of flowering by photoperiod (fig. S11). Analysis of the putative zinc fingers confirmed the classification based on the CCT domains (fig. S12). CO-like proteins from Groups I and II have one or two B-box zinc fingers, whereas the ZCCT proteins showed one C_2H_2 zinc finger. Group IV zinc fingers were similar, although not identical, to those from the *ZCCT* proteins (fig. S12).

These results suggest that the ancestor of the *ZCCT* and Group IV proteins originated in the grasses and that the ZCCT proteins diverged substantially in the temperate cereal species adapted to the cold regions. The divergence of the ZCCT pro-
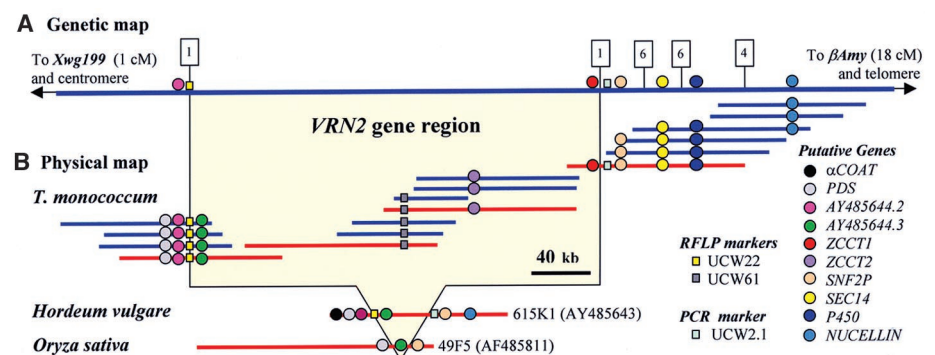

Fig. 1. (**A**) Genetic map of the *VRN2* region on chromosome 5A^m of *T. monococcum*, based on 5698 gametes. The number of crossovers in the critical recombinant plants is indicated in the boxes. (**B**) Physical map of the wheat *VRN2* region in *T. monococcum* and in colinear regions from barley and rice. BAC clones indicated in red have been sequenced (438,828 bp, AY485644). The order of BAC clones from left to right is 374A18, 94E8, 304H18, **258C22**, **301G15**, 615O6, 650N20, **405L8**, 271O11, 275P20, 157P20, **455C17**, 322L23, 702K8, 32A1, 533H16, and 324G2 (bold letters indicate sequenced BACs). Additional information for the markers used in this figure is available in the supporting online material.

teins might have been favored by a duplication of the ancestral Group IV protein in the temperate cereals. This is suggested by the absence of *ZCCT* orthologs in rice in the colinear region between *AY485644.3* and *SNF2P* (Fig. 1).

Variation of the RNA levels of the candidate genes during vernalization. The RNA levels of the three genes completely linked to *VRN2* were investigated during vernalization. RNA amounts of the *AY485644.3* gene were not affected by vernalization (Fig. 2A) and were similar in spring and winter genotypes. Numerous Triticeae expressed sequence tags (ESTs) from different complementary DNA (cDNA) libraries showed similarity to *AY485644.3* ($E < e^{-100}$), suggesting relatively high messenger RNA (mRNA) levels in different tissues.

In contrast, the absence of ESTs corresponding to the *ZCCT* genes in the extensive wheat and barley collections suggested low transcript levels. *ZCCT1* and *ZCCT2* transcripts were detected by reverse transcription (RT)–PCR in the leaves before but not after vernalization (Fig. 2A). The mRNA levels of *ZCCT1* and *ZCCT2* in diploid wheat were quantified with TaqMan systems (*13*) (figs. S13 and S14) and with *ACTIN* and *UBIQUITIN* as endogenous controls (*5*). A progressive decrease in *ZCCT1* (Fig. 2B) and *ZCCT2* transcripts (fig. S15) was observed in the leaves during vernalization. Control winter plants kept at room temperature maintained relatively high *ZCCT* RNA levels. *ZCCT* transcription was not restored after the plants were removed from the cold (4°C) room after 6 weeks of vernalization (Fig. 2B). Down-regulation of *ZCCT1* after vernalization was also confirmed in the common winter wheat variety Jagger (*18*).

The down-regulation of the *ZCCT* genes during vernalization was concomitant with an increase in wheat *VRN1* (the same as to *AP1*) transcription (Fig. 2B). These opposite transcription profiles are consistent with the epistatic interactions between *VRN1* and *VRN2* (*2*, *5*). *ZCCT1* transcripts were present in the apices from the unvernalized winter plants but were not detected after vernalization (Fig. 2C). *VRN1* transcripts in the apices showed the same pattern as in the leaves, being induced after vernalization (Fig. 2C). Using the same RNA samples, we did not detect transcripts of *ZCCT2*. These results suggested that either *ZCCT2* was not expressed in the apices or that its transcription level was below our detection threshold. Because apices are the critical points for the transition between the vegetative and reproductive phases, these observations suggested that *ZCCT1* was a better candidate for *VRN2* than was *ZCCT2*.

Allelic variation of candidate genes among cultivated *T. monococcum* accessions. *ZCCT1* transcription was down-regulated during vernalization in both winter G3116 and spring DV92 plants, sug-
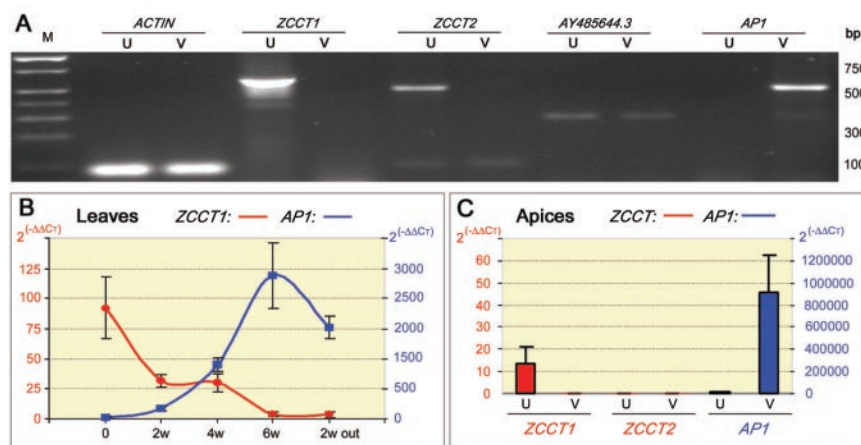

Fig. 2. (A) RT-PCR from leaves of unvernalized (U) or vernalized (V) G3116 winter wheat plants. RNA samples from the vernalized plants (6 weeks at 4°C) were collected 5 days after the plants were returned to room temperature. Among the three genes completely linked to *VRN2*, RNA levels of *ZCCT1* and *ZCCT2* were down-regulated by vernalization and those of *AY485644.3* were not affected by vernalization. In the same cDNA samples, *AP1* RNA levels were up-regulated by vernalization. M, molecular-weight DNA marker. **(B and C)** Quantitative PCR of leaves and apices. **(B)** Transcript levels of *ZCCT1* (red scale) and *AP1* (blue scale) relative to *UBIQUITIN* in G3116; averages of five plants ± SE are shown. On the x axis, 0 indicates the time before exposure to 4°C; w, weeks at 4°C; 2w out, 2 weeks at room temperature after vernalization. **(C)** Transcript levels of *ZCCT1*, *ZCCT2*, and *AP1* (wheat *VRN1*) relative to *ACTIN* in G3116, showing the averages of three pools of apices from five plants each ± SE. U, unvernalized; V, 3 to 5 days at room temperature after 6 weeks of vernalization. Units are values linearized with the $2^{(-\Delta\Delta CT)}$ method, where CT is the threshold cycle.

gesting that the differences in growth habit were not caused by differences in the transcriptional regulation of *ZCCT1*. To test this hypothesis, we compared the sequences of the promoter and coding regions from the three *VRN2* candidate genes between spring and winter accessions of cultivated *T. monococcum* (table S1).

We observed no differences in the AY485644.3 protein between *vrn2*-spring accession DV92 and *Vrn2*-winter germ plasm PI355532 and PI277133 (accession nos. AY485962 and AY485961). Similarly, no differences were found in the predicted ZCCT2 proteins between *vrn2*-spring accession DV92 and *Vrn2*-winter germplasm PI272561 and PI277133 (AY485976 and AY485975). In addition, no differences were found between DV92 and winter accession PI272561 in the first kilobase of the promoter or in the 763 bp of the 3′ end region of the *ZCCT2* gene (supporting online text). These results suggested that the differences in vernalization requirement were not caused by differences in the coding sequences of these two genes or in the regulatory sequences of *ZCCT2*.

No differences were found in the promoter region of *ZCCT1* between DV92 and winter accession PI272561 (*13*). However, comparison of the *ZCCT1* coding region between DV92 and 16 *T. monococcum* accessions with a winter growth habit (table S1) provided good evidence that *ZCCT1* was the *VRN2* gene. The spring accession DV92 carried a point mutation at position 35 of the CCT domain that replaced an arginine (R) amino acid with a tryptophan (W).

This R is conserved in all of the ZCCT proteins (fig. S10) and in all of the CO-like proteins from *Arabidopsis*, rice, and barley (*17*). A point mutation at the same position in the CCT domain of CO in *Arabidopsis* ethyl methanesulfonate mutant co-7 did not affect the nuclear localization of the CO protein but produced a severe effect on flowering time (*16*). Kurup *et al.* (*19*) suggested that the CCT domain might be involved in protein-protein interactions and that a mutation within this domain can disrupt these interactions. The conservation of the 35-R amino acid in all the CCT domains and the strong effect of its mutation on flowering time in *Arabidopsis* suggest that this amino acid is essential for the correct function of the CCT domain and that the point mutation observed in DV92-*ZCCT1* is the likely cause of its spring growth habit.

The R/W mutation in DV92 created an Nco I restriction site (fig. S3) that was absent in the wild allele. This polymorphism was used to screen a germplasm collection of 65 accessions of cultivated *T. monococcum* from different parts of the world (table S1). The R/W mutation was absent in all 16 accessions with a winter growth habit, but it was present in 22 of the 49 spring accessions (table S1). Screening of the remaining 27 spring accessions by hybridization with *ZCCT1* showed that 17 accessions had a complete deletion of *ZCCT1* and *ZCCT2* (supporting online text). Seven of the ten remaining spring accessions showed deletions in the *VRN1* promoter that explained their spring growth habit (*5*). The spring growth habit of the last three accessions remains unexplained. In summary, the
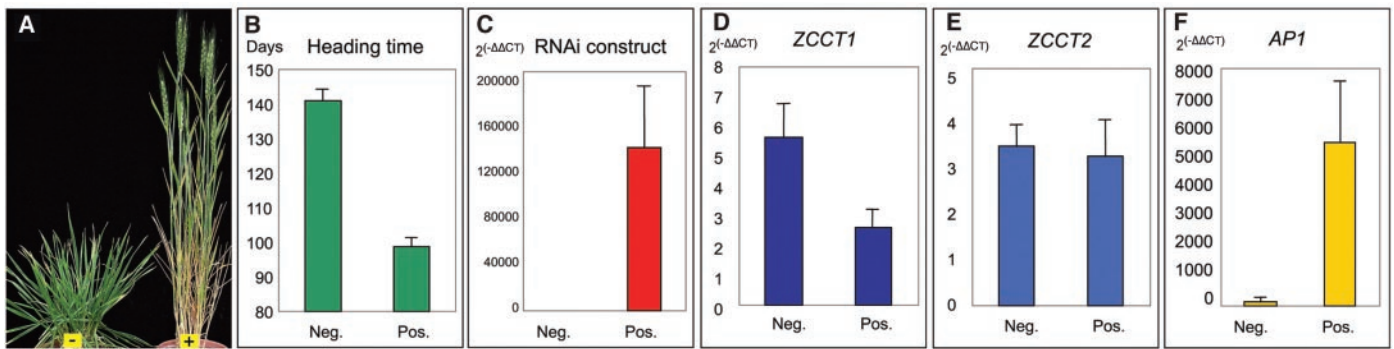
Fig. 3. (**A**) Transgenic Jagger T_1 plants segregating for the presence (+) and absence (–) of the RNA interference construct for *ZCCT1* and flowering time. (**B**) Average heading date of T_1 plants with (Pos., 31 plants) and without (Neg., 11 plants) the transgene. (**C** to **F**) Average RNA level of (C) the RNAi construct and average endogenous RNA levels of (D) *ZCCT1*, (E) *ZCCT2*, and (F) *AP1*, in eight positive and eight negative T_1 plants from the progeny of the early flowering T_0 plant. Units are values linearized with the $2^{(-\Delta\Delta CT)}$ method. Error bars indicate 1 SEM.

mutations or deletions at the *ZCCT1* gene and the *VRN1* promoter described so far were sufficient to explain the spring growth habit of 46 out of the 49 cultivated *T. monococcum* accessions we analyzed (table S1).

Allelic variation in barley. The absence of *ZCCT* genes in the orthologous BAC from spring barley variety Morex (Fig. 1) suggested that this variety carries a recessive *vrn2* allele. Hybridization of Xba I–digested, barley genomic DNA with a wheat *ZCCT1* probe showed no hybridization in Morex but three RFLP fragments in winter *H. spontaneum*. The analysis of 102 F_2 plants from a cross between the spring variety Morex and the winter accession of *H. spontaneum* showed that all the F_2 plants homozygous for the deletion had a spring growth habit. In addition, the three RFLP fragments were completely linked to *VRN2* flanking gene *SNF2P*, demonstrating that Morex has a recessive *vrn2* allele completely linked to the *ZCCT* deletion.

To study the distribution of the deletion of the *ZCCT* genes in barley and its association with the *vrn2* allele, we screened a collection of 85 barley varieties from different parts of the world that were previously characterized genetically for their vernalization alleles [20]. Hybridization of Southern blots of DNA from these varieties with the wheat *ZCCT1* probe showed the presence of the *ZCCT* genes in the 23 winter barley varieties and complete deletion of all *ZCCT* genes in 61 *vrn2*-spring barley varieties [21]. Spring barley variety Fan (*vrn2*) showed only one *ZCCT* gene, indicating a different deletion [21].

Validation of *ZCCT1* as *VRN2* by RNA interference (RNAi) transgenic wheats. Transformation experiments were performed in winter hexaploid wheat variety Jagger, because it is currently not possible to efficiently transform diploid *T. monococcum*. Transformation was performed by bombardment with an RNAi construct that included a 347-bp segment from the *T. monococcum ZCCT1* gene [13]. We identified three independent transgenic plants by PCR [13], but only one of them showed the expect-

ed acceleration of flowering relative to the negative controls and was analyzed further.

We self-pollinated the early-flowering transgenic T_0 plant and determined the presence or absence of the transgene in 42 plants from the T_1 progeny by Southern blots. The plants carrying the transgene flowered on average 42 days earlier than the negative plants ($P < 0.001$) (Fig. 3, A and B). Quantitative PCR analysis of eight negative and eight positive transgenic T_1 plants (Fig. 3, C to F) showed reduction of the endogenous RNA levels of *ZCCT1* ($P < 0.05$) (Fig. 3D) but not of *ZCCT2* ($P = 0.79$) (Fig. 3E). The positive transgenic T_1 plants showed higher *AP1* RNA levels ($P < 0.001$) (Fig. 3F). This experiment confirmed that the reduction of the RNA level of *ZCCT1* is associated with the acceleration of flowering time and that RNAi can be used successfully in polyploid wheat, which carries multiple homologous copies of *ZCCT1*. This experiment also demonstrated that *VRN2* regulates flowering by vernalization in polyploid winter wheats, despite observations of allelic variation at this locus in diploid but not polyploid wheat [4].

The vernalization response in temperate cereals. The complete linkage between *ZCCT1* and *VRN2* in a large mapping population, its gradual and stable transcriptional down-regulation by vernalization, its opposite transcription profile to *VRN1*, the association between natural allelic variation at *ZCCT1* and spring growth habit, and the acceleration of flowering time by RNAi of *ZCCT1* transcripts all demonstrate that *ZCCT1* is *VRN2*.

The *ZCCT1* gene belongs to a different family of transcription factors than the *Arabidopsis* MADS-box gene *FLC* but has an analogous function. Both genes are dominant repressors of flowering down-regulated by vernalization. Similarities between ZCCT1 and *Arabidopsis* proteins are restricted to the conserved CCT domains present in CO and CO-like proteins. However, the CCT domains from the *ZCCT* genes belong to a group that does not include any *Arabidopsis* protein (fig. S11).

An additional difference between wheat and *Arabidopsis* is the frequent association between natural differences in growth habit and allelic variation at the *AP1* locus in wheat [5] but not in *Arabidopsis*. Even in the extensive collection of *Arabidopsis* mutants, there are no reports of differences in vernalization requirement associated with the *AP1* gene.

Based on the previous observations, and the knowledge that temperate grasses evolved from subtropical primitive grasses that likely had no vernalization requirement [22], we conclude that *Arabidopsis* and the temperate grasses developed different vernalization pathways, including different genes down-regulated by vernalization (*ZCCT1* and *FLC*) and similar genes with different regulatory profiles (*AP1*). The development of a vernalization response was an important step for the adaptation of the grasses to the cold regions. In most of the wild Triticeae species, vernalization accelerates flowering, suggesting that the winter growth habit is the ancestral state in this group of species. However, these winter species retained the capacity to generate spring forms by loss of function mutations at two main vernalization loci. Independent mutations at these loci were maintained by natural selection in the wild species and by a strong selection pressure in the domesticated wheat and barley varieties. These results suggest that the wide adaptability of temperate cereals was favored by a flexible regulation system of flowering time.

References and Notes

1. R. Takahashi, S. Yasuda, in *Proceedings of the 2nd International Barley Genetics Symposium*, Pullman, WA, 6 to 11 July 1969, R. A. Nilan, Ed. (Washington State Univ. Press, Pullman, 1971), pp. 388–408.
2. G. E. Tranquilli, J. Dubcovsky, *J. Hered.* **91**, 304 (2000).
3. D. A. Laurie, N. Pratchett, J. H. Bezant, J. W. Snape, *Genome* **38**, 575 (1995).
4. J. Dubcovsky, D. Lijavetzky, L. Appendino, G. Tranquilli, *Theor. Appl. Genet.* **97**, 968 (1998).
5. L. Yan *et al.*, *Proc. Natl. Acad. Sci. U.S.A.* **100**, 6263 (2003).
6. S. Gazzani, A. R. Gendall, C. Lister, C. Dean, *Plant Physiol.* **132**, 1107 (2003).
7. S. D. Michaels, R. M. Amasino, *Plant Cell* **11**, 949 (1999).
8. C. C. Sheldon *et al.*, *Plant Cell* **11**, 445 (1999).

9. U. Johanson *et al.*, *Science* **290**, 344 (2000).
10. S. B. Sung, R. M. Amasino, *Nature* **427**, 159 (2004).
11. A. R. Gendall, Y. Y. Levy, A. Wilson, C. Dean, *Cell* **107**, 525 (2001).
12. Y. Y. Levy, S. Mesnage, J. S. Mylne, A. R. Gendall, C. Dean, *Science* **297**, 243 (2002).
13. Materials and methods are available as supporting material on *Science* Online.
14. D. Lijavetzky *et al.*, *Genome* **42**, 1176 (1999).
15. J. Putterill, F. Robson, K. Lee, R. Simon, G. Coupland, *Cell* **80**, 847 (1995).
16. F. Robson *et al.*, *Plant J.* **28**, 619 (2001).
17. S. Griffiths, R. P. Dunford, G. Coupland, D. A. Laurie, *Plant Physiol.* **131**, 1855 (2003).
18. L. Yan, A. Loukoianov, J. Dubcovsky, unpublished data.
19. S. Kurup, H. D. Jones, M. J. Holdsworth, *Plant J.* **21**, 143 (2000).
20. R. Takahashi, "Catalogue of the barley germplasm preserved in Okayama University" (Research Institute for Bioresources, Okayama University, Okayama, Japan, 1983).
21. C.-L. Chen, thesis, University of California, Davis (2002).
22. W. D. Clayton, S. A. Renvoize, *Genera Graminum: Grasses of the world* (Royal Botanic Gardens, Kew, London, 1986).
23. We thank X. Zhang, A. Sanchez, J. Lin, R. Shao, and C. S. Busso for excellent technical assistance; C. M. Leutenegger for his help with the TaqMan systems; V. Chandler for the pMCG161 vector; the U.S. National Small Grain Collection for the *T. monococcum* seeds; and Okayama University (Japan) and A. Kleinhofs for the barley seeds. Supported by the U.S. Department of Agriculture, National Research Initiative grant nos. 2000-1678 and 2003-00929, and by NSF Plant Genome Research Program no. 9975793.

REPORTS

Elastomeric Transistor Stamps: Reversible Probing of Charge Transport in Organic Crystals

Vikram C. Sundar,[1]*† Jana Zaumseil,[1]*‡ Vitaly Podzorov,[2]*
Etienne Menard,[3] Robert L. Willett,[1] Takao Someya,[1]§
Michael E. Gershenson,[2] John A. Rogers[3]‖

We introduce a method to fabricate high-performance field-effect transistors on the surface of freestanding organic single crystals. The transistors are constructed by laminating a monolithic elastomeric transistor stamp against the surface of a crystal. This method, which eliminates exposure of the fragile organic surface to the hazards of conventional processing, enables fabrication of rubrene transistors with charge carrier mobilities as high as ~15 cm²/V·s and subthreshold slopes as low as 2 nF·V/decade·cm². Multiple relamination of the transistor stamp against the same crystal does not affect the transistor characteristics; we exploit this reversibility to reveal anisotropic charge transport at the basal plane of rubrene.

Basic scientific interest and potential applications in large-area, flexible electronic systems motivate research in the field of organic semiconductors (*1–4*). Despite a substantial body of work aimed at understanding charge transport in these materials (*5–11*), a well-developed, microscopic description is still lacking. It is for this reason that studies of organic single crystals, in which grain boundaries are eliminated and concentration of charge traps is minimized, are important. A primary experimental difficulty is that the field-effect structures that are needed for these measurements require fabrication steps that can disrupt molecular order and bonding, generate interfacial trapping sites, create barriers to charge injection, and cause other unwanted changes to these fragile molecular systems (*12*). There is, therefore, a strong need for nondestructive, reversible methods to fabricate field-effect transistors (FETs) based on single crystals of organic semiconductors in a way that reveals intrinsic properties and removes processing-related effects.

In our technique, the transistor circuitry (the source-drain-gate electrodes and gate dielectric) is fabricated on a flexible elastomeric substrate, which, at the final stage, is bonded to the surface of organic crystal by van der Waals forces. In this respect, our technique is similar to the fabrication of organic FETs by laminating an organic crystal against a silicon wafer with predeposited electrodes (*8, 9*). The main advantage of both elastomeric and Si-based stamp techniques is

obvious: They eliminate the need for deposition of metals and dielectrics directly onto a very fragile organic surface. The elastomeric technique, however, has two important advantages compared with the Si-based technique. First, in contrast with Si-based substrates that require very thin (~1 μm) and bendable crystals (which are prone to strain-induced defects), the elastomeric stamps are compatible with much thicker (up to a few mm) and rigid crystals, as the flexible elastomeric surface and the ductile Au contacts adjust easily to the crystal shape. Second, the elastomeric stamp technique is nondestructive and reversible. The contact between the stamp and organic crystals can be reestablished many times without affecting the transistor characteristics. We exploited this experimental capability to explore the dependence of the field-effect mobility on the orientation of the transistor channel relative to the crystallographic axes and observed for the first time a strong anisotropy of the field-effect mobility within the *a-b* plane of single crystals of rubrene.

Figure 1 shows the transistor stamps used and outlines the steps of device fabrication. A flexible elastomer, polydimethylsiloxane (PDMS), is used as a substrate on which the transistor stamp is constructed (*13*). Gate and source-drain electrodes (Ti/Au) are evaporated through shadow masks and are separated by an additively transferred thin film (2 to 4 μm) of PDMS (*14*). The flexibility of both the dielectric and the substrate (and therefore all the gold electrodes in these transistor stamps) enables assembly of devices through simple lamination of the organic crystal and elastomeric stamp surface (*13*). Slight pressure applied to one edge of the crystal initiates contact with the stamp (Fig. 1B); van der Waals forces then spontaneously cause a "wetting" front to proceed across the surface of the crystal (Fig. 1B, center frame). The low free-surface energy of PDMS favors the progression of such a wetting front (*15, 16*) across the flat surfaces of organic crystals. The absence of interference fringes (as observed

[1]Bell Laboratories, Lucent Technologies, Murray Hill, NJ 07974, USA. [2]Department of Physics and Astronomy, Rutgers University, Piscataway, NJ 08854, USA. [3]Department of Materials Science and Engineering, Department of Chemistry, Beckman Institute and Seitz Materials Research Laboratory, University of Illinois, Urbana-Champaign, IL 61801, USA.

*These authors contributed equally to this work.
†Present address: IBM, Yorktown Heights, NY 10598, USA.
‡Present address: Cavendish Laboratory, Cambridge CB3 0HE, UK.
§Present address: University of Tokyo, Tokyo 264-8505, Japan.
‖To whom correspondence should be addressed. E-mail: jrogers@uiuc.edu